The Impact of Spark-igniting Configuration on Detonation Onset in a Rapid Compression Machine

Yingdi Wang [a], Wei Liu [a], Yunliang Qi [a,b], Zhi Wang [a]
[a] State Key Laboratory of Automotive Safety and Energy, Tsinghua University
Beijing, China
[b] Graduate Aerospace Laboratories, California Institute of Technology
Pasadena, USA

1 Introduction

Super-knock is one of the major obstacles for further improving power density in highly boost engines. Different from conventional knock, which is originated from end gas auto-ignition, detonation occurs in super-knock conditions [1]. However, the detonation initiation mechanism still remains unclear. The acoustic coupling theory [2] has been evidenced by experimental observation, i.e., shock wave capturing by schlieren and high speed imaging [3-5]. Above all, a pre-ignition followed by coupling of shock wave and auto-ignition is the prerequisite of detonation onset [6].

To suppress auto-ignition, flame acceleration by novel ignition configurations is considered. As reported by Chen et al., a competition between short residual time and higher p,T of unburned region need further discussion [7]. End gas thermodynamic condition increases with faster flame propagation, while less time is left for auto-ignition. Therefore, contradictory trends of knock intensity are obtained with increasing burned mass fraction (BMF) [8, 9]. A shift from isochoric to isobaric combustion due to heat loss is proposed by Yu et al. to interpret the complex impact of BMF.

In practical application, multiple spark plugs are tried to increase thermal efficiency with knock suppression [10]. Thus, along with previous studies [11, 12], manually triggered spark plugs are utilized to induce detonation in a rapid compression machine (RCM). Different spark igniting configurations, including a side or central distributed spark plug and circumferential distributed spark plugs, are compared to investigate the impact of BMF and burning velocity on detonation onset.

2 Experimental Setup

2.1 Rapid compression machine

Correspondence to: qiyl@caltech.edu

Experiments were conducted in TU-RCM. A detailed description can be found in [13, 14]. Briefly, as shown in Figure 1, a quartz window was utilized to offer an optical access from the end wall. The images were recorded using a high speed camera (Photron SA-X2) at frame rate 288000 fps (frame interval of 3.47 μs). Twelve even-distributed spark plugs were flush mounted on the circumferential side wall of combustion chamber to realize multi-igniting simultaneously, where variable number of spark plugs were activated in each experiment. Besides, a single spark plug with extended electrode was used to realized central distributed spark. The spark timing was controlled within 3 ms after the end of compression (EOC) according to cylinder pressure.

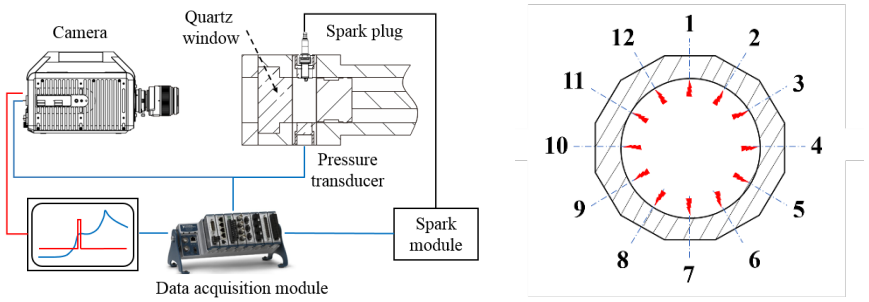

Figure 1. The schematic of optical TU-RCM (left) and circumferential distributed spark plugs (right)

2.2 Mixtures and conditions

The stoichiometric iso-octane/'air' mixture was used as gasoline surrogate, where argon was utilized to realize different temperature at EOC, shown in Table 1.

Table 1: Stoichiometric iso-octane/'air' mixture composition and experimental conditions

No.	φ	molar fraction / %				p_{eoc} / MPa	T_{eoc} / K
		iC_8H_{18}	O_2	N_2	Ar		
1	1.0	1.65	20.66	77.69	/	11~26	613
2	1.0	1.65	20.66	44.63	33.06	11~15	668
3	1.0	1.65	20.66	52.89	24.79	11~15	738

Different ignition regimes were observed under a single spark ignition condition, including detonation and deflagration, shown in Figure 2. The energy density U is defined as

$$U = \rho H_u = H_u p_f W_f / RT \quad (1)$$

where p_f, W_f represents the partial pressure and molar weight of the fuel respectively. The transition occurred at around $p = 14$ bar, $U = 23$ MJ/m^3 with a side spark plug while the central distributed form appears to be more resistant to detonation onset. Then, the experiments using multiple spark plugs were conducted under similar thermodynamic conditions.

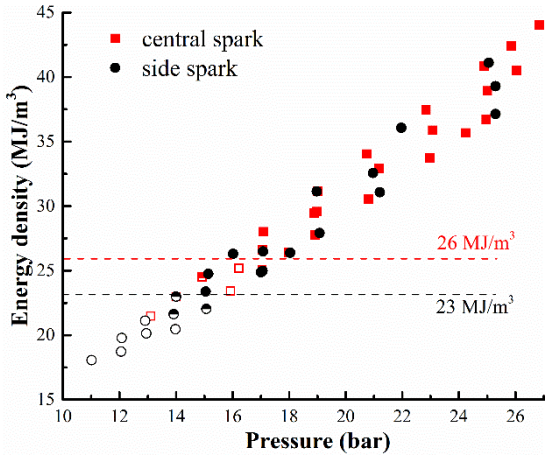

Figure 2. Energy density distribution with elevated pressure using a single side or central spark plug, p = 11~26 bar, T = 610~740 K (solid scatters represent detonation onset while hollow ones represent detonation failure)

3 Results

Different ignition phenomena, especially the transition from end gas auto-ignition to detonation, are shown in Figure 3 with multiple spark plugs. Three adjacent images are demonstrated in sequence for each case, where the last two are presented with background subtraction. The supersonic reaction front with extremely high luminosity is supposed to be detonation. Pressure oscillation amplitude is also depicted in Figure 4. The detonation cases are clearly distinguished by oscillation intensity, marked as solid scatters.

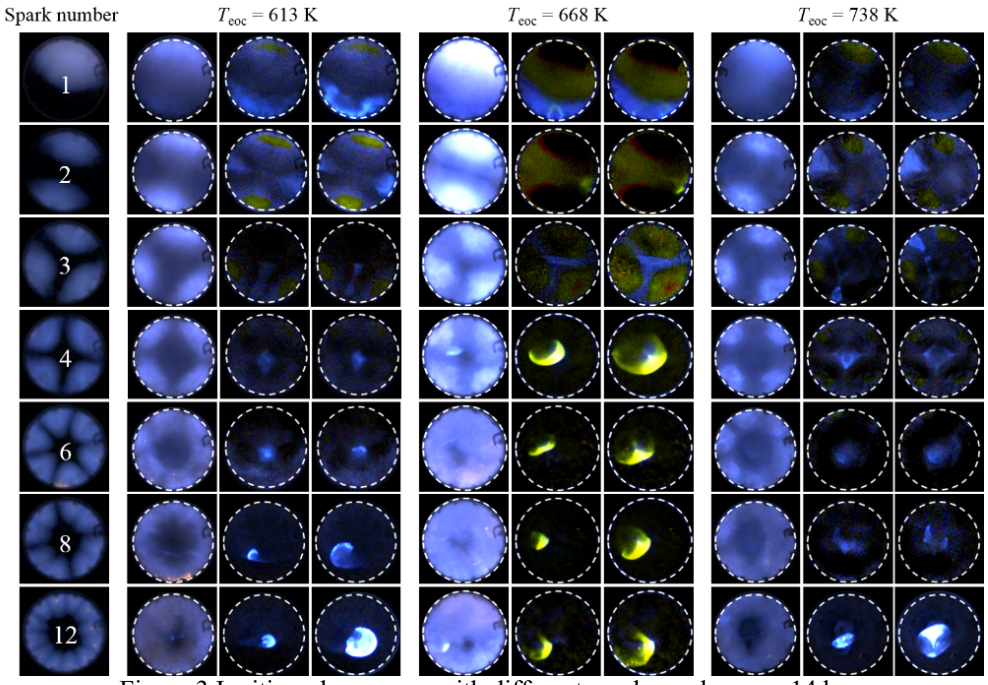

Figure 3 Ignition phenomena with different spark number, p = 14 bar
(background subtraction is utilized to emphasize the detonation onset)

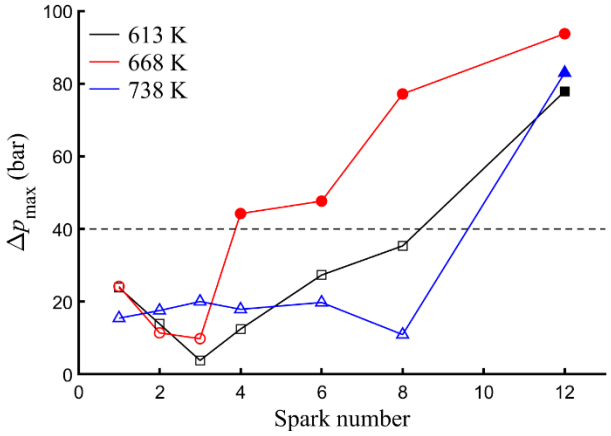

Figure 4. Pressure oscillation under different spark number conditions, p=14 bar

(solid scatters represent detonation onset while hollow ones represent detonation failure)

Obviously, the knock intensity is not proportional to burning velocity. In current work, a minimum value is achieved with around 3 spark plugs. Detonation tendency becomes stronger rapidly with more spark plugs. It means an optimal burning velocity exists for knock suppression.

The BMF at the instant of strong auto-ignition or detonation onset, calculated by pressure ratio based on equilibrium p_{eq}, is shown in Figure 5. Under 613 K, the BMF demonstrates a 'hill' curve instead of the monotone increasing trend under higher temperature. It denotes that with spark number increasing (more than 6), the unburned gas tends to ignite earlier and be able to transit into detonation. Thus, ignition delay time evolutions of unburned gas during the flame propagation are shown in Figure 6 to further discuss this issue. Since the unburned gaseous mixture are located in the central region, isentropic correlation is applied to calculate the temperature from pressure with neglect of the heat release of low temperature reactions. The detonation onset under 613 K is within the negative temperature coefficient (NTC) region, while the others get across the region. Therefore, the low temperature reactions may be responsible for the advance of unburned gas auto-ignition.

$$\mathrm{BMF} = (p - p_{\mathrm{eoc}})/(p_{\mathrm{eq}} - p_{\mathrm{eoc}}) \tag{2}$$

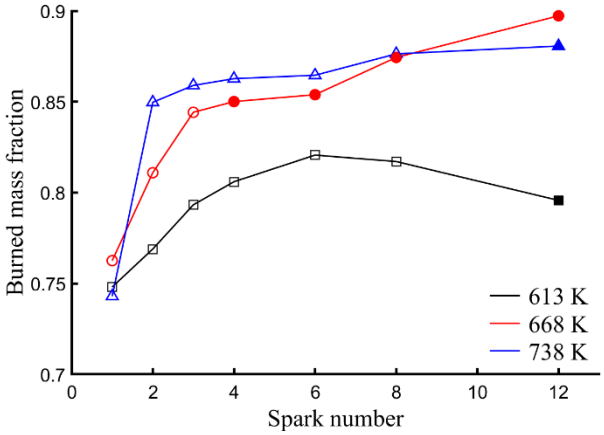

Figure 5. BMF under different spark number conditions, p=14 bar

(solid scatters represent detonation onset while hollow ones represent detonation failure)

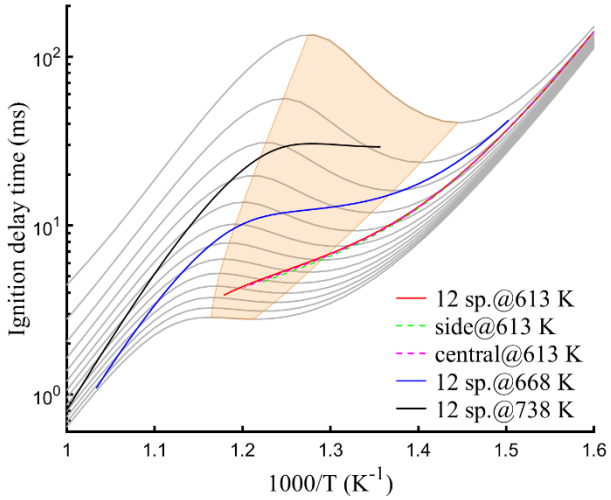

Figure 6. Ignition delay time evolutions of different spark-igniting configuration and termperature, p=14 bar
gray lines are calculated results using 0-D model with pressure ranging from 10~70 bar with a 5 bar step

Moreover, pressure traces using different spark-igniting configurations are compared in Figure 7. Burning velocity of the case using central distributed spark plug is between 2 and 3 circumferential forms. The minimum knock intensity is realized thereby without detonation occurrence. Thus, a moderate burning velocity is desired to suppress detonation onset.

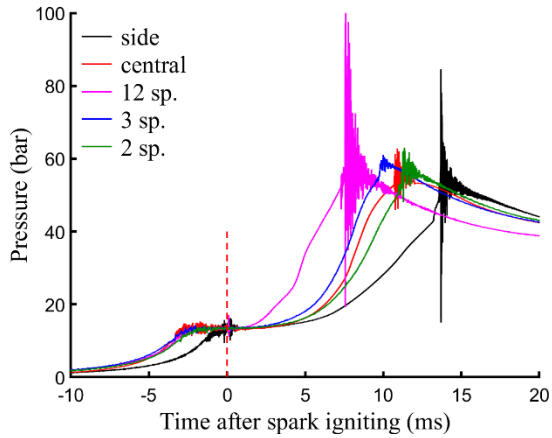

Figure 7. Pressure comparison between different spark-igniting configurations, T=613 K, p=14 bar

4 Conclusions

In present study, a combination of experimental and numerical method is used to analyze the impact of different spark igniting configurations on detonation onset.

First, when using the circumferential configuration, the oscillation intensity is not proportional to spark number (burning velocity). An optimal spark number of 3 is reported with best detonation suppression effect. With spark number further increase, the detonation tendency becomes even stronger than using a single spark plug. It is worth noticing that despite of the detonation onset, the mechanical impact by pressure oscillation is dissipated by a burned gas layer near wall.

In addition, the burned mass fraction does not necessarily change monotonously with spark number increase, owing to the NTC behavior of the fuel. When the ignition delay time evolutions of unburned gas terminate within the NTC region, the BMF demonstrates a contratry trend.

Above all, a moderate burning velocity is required for detonation suppression based on the comparison of different spark-igniting configurations.

References

[1] Z. Wang, Y. Qi, X. He, J. Wang, S. Shuai, C.K. Law. (2015). Analysis of pre-ignition to super-knock: Hotspot-induced deflagration to detonation. Fuel. 144: 222-227.

[2] X.J. Gu, D.R. Emerson, D. Bradley. (2003). Modes of reaction front propagation from hot spots. Combustion and Flame. 133: 63-74.

[3] J. Pan, C.G.W. Sheppard, A. Tindall, M. Berzins, S.V. Pennington, J.M. Ware. (1998). End gas inhomogeneity, autoignition and knock. SAE Technical Papers.

[4] M. Pöschl, T. Sattelmayer. (2008). Influence of temperature inhomogeneities on knocking combustion. Combustion and Flame. 153: 562-573.

[5] U. Spicher, H. Kröger, J. Ganser. (1991). Detection of knocking combustion using simultaneously high-speed schlieren cinematography and multi optical fiber technique. SAE Technical Papers.

[6] Z. Wang, H. Liu, T. Song, Y. Qi, X. He, S. Shuai, J. Wang. (2015). Relationship between super-knock and pre-ignition. International Journal of Engine Research. 16: 166-180.

[7] Y. Chen, R. Raine. (2015). A study on the influence of burning rate on engine knock from empirical data and simulation. Combustion and Flame. 162: 2108-2118.

[8] L.S. Kagan, P.V. Gordon, G.I. Sivashinsky. (2012). A minimal model for end-gas autoignition. Combustion Theory and Modelling. 16: 1-12.

[9] A. Robert, S. Richard, O. Colin, T. Poinsot. (2015). LES study of deflagration to detonation mechanisms in a downsized spark ignition engine. Combustion and Flame. 162: 2788-2807.

[10] B. Nandakumar Kartha, S. Vijaykumar, P. Reddemreddy. (2016). Thermodynamic Split of Losses Analysis of a Single Cylinder Gasoline Engine with Multiple Spark Plug - Ignition Coil Configurations. SAE Technical Papers. 2016-November:

[11] Y. Wang, Y. Qi, S. Xiang, R. Mével, Z. Wang. (2018). Shock wave and flame front induced detonation in a rapid compression machine. Shock Waves. 28: 1109-1116.

[12] Z. Wang, Y. Qi, H. Liu, P. Zhang, X. He, J. Wang. (2016). Shock wave reflection induced detonation (SWRID) under high pressure and temperature condition in closed cylinder. Shock Waves. 26: 687-691.

[13] Y. Qi, X. He, Z. Wang, J. Wang. (2014). Frequency domain analysis of knock images. Measurement Science and Technology. 25:

[14] H. Di, X. He, P. Zhang, Z. Wang, M.S. Wooldridge, C.K. Law, C. Wang, S. Shuai, J. Wang. (2014). Effects of buffer gas composition on low temperature ignition of iso-octane and n-heptane. Combustion and Flame. 161: 2531-2538.